

NUMERICAL ANALYSIS OF ENTANGLEMENT PROPERTIES OF DENSITY MATRICES IN $C^2 \otimes C^2$ SYSTEMS

RUBENS VIANA RAMOS

*Departamento de Engenharia de Teleinformática – Universidade Federal do Ceará - DETI/ UFC
C.P. 6001 – Campus do Pici - 60455-760 Fortaleza-Ce Brasil*

ANDERS KARLSSON

*Department of Microelectronics and Information Technology, Royal Institute of Technology (KTH)
Electrum 229, 164 40 Kista, Sweden*

Received: October 16, 2001

Revised: February 19, 2002

Quantum entanglement is an enigmatic and powerful property that has attracted much attention due to its usefulness in new ways of communications, like quantum teleportation and quantum key distribution. Much effort has been done to quantify entanglement. Indeed, there exist some well-established separability criterion and analytical formulas for the entanglement of bipartite systems. In both, the crucial element is the partial transpose of the density matrix. In this paper, we show numerically that one can also have information about the entanglement of bipartite state, in $C^2 \otimes C^2$, without looking at the partial transpose. We furthermore study properties of disentanglement operation, as well as properties of the relative entropy.

Keywords: Density Matrix, quantum entanglement measures and separability criterion
Communicated by: B Kane & C Williams

1. Introduction

Entanglement is the physical property fundamental for development of quantum information processing such as quantum cryptography (based on non-locality) and quantum teleportation both at the heart of the recently created quantum information theory. The density matrix of a quantum state contains all information available on all possible future developments of a quantum state. Indeed, the separability (if a state is entangled or not) as well as the quantification of the entanglement of composite quantum systems are obtained using the density matrix, through its partial transpose [1-6]. In this article we propose a different approach in the treatment of the density matrix to obtain information about the entanglement of bipartite states in $C^2 \otimes C^2$. We separate the density matrix in a sum of two other matrices, where the first one represents a disentangled quantum state stemming from the individual parts of the composite system, and the second one, with null trace, is the rest matrix. Our goal is to find, numerically (in order to avoid long and tedious calculus), relations between the properties of the rest matrix and the entanglement properties of the overall system. In the following two sections we do a review of the separability criterion and entanglement measures for bipartite states. In the fourth section we analyse properties of the matrix R that can be seen as hints of entanglement presence. We show simulations and comment our results. In section 5, we consider our decomposition of the density matrix in the procedure of disentangling, which erase the entanglement preserving the individual subsystems. Finally, in the last section, we investigate the usefulness of the relative entropy between an entangled state and a disentangled state with the same individual parts.

2. Separability Criterion

The separability criterion for 2x2 and 2x3 systems was proposed by Peres and the Horodecki family in [1,2]. It states that if the partial transpose of the density matrix does not have negatives

eigenvalues then the state is separable otherwise it is entangled. Explicitly, let Γ be the density matrix of a bipartite system with density matrices of the individual parts $\rho_a = Tr_b(\Gamma)$ and $\rho_b = Tr_a(\Gamma)$, where $Tr_{a(b)}$ stands for the partial trace with respect to subsystem $a(b)$. The elements of Γ can be given as:

$$\Gamma_{m\mu, n\nu} = \langle A_m, B_\mu | \Gamma | A_n, B_\nu \rangle \quad (1)$$

where $\{A_m\}$ and $\{B_\mu\}$ are (arbitrary) orthonormal basis, in the Hilbert space, for the individual systems, A and B , respectively. Using this representation, the partial transpose relative to the A system is given by [1,2]:

$$\Gamma_{m\mu, n\nu}^{T_A} = \Gamma_{n\mu, m\nu} \quad (2)$$

If Γ is separable (disentangled) it has the form:

$$\Gamma = \sum_i p_i \rho_a^i \otimes \rho_b^i = \sum_i p_i (\rho_a^i)_{mn} (\rho_b^i)_{\mu\nu} \quad (3)$$

$$\sum_i p_i = 1 \quad (4)$$

In this case, Eq. (2) is equivalent to:

$$\Gamma^{T_A} = \sum_i p_i (\rho_a^i)^T \otimes \rho_b^i \quad (5)$$

The Peres-Horodecki criterion is a binary condition: The partial transpose has or has not any negative eigenvalue? A quantitative version of this criterion was proposed by Vidal and Werner by using a new quantity, based on the trace norm of the partial transpose, called negativity [3]:

$$N_e(\Gamma) \equiv \frac{\|\Gamma^{T_A}\|_1 - 1}{2} \quad (6)$$

$$\|\Gamma^{T_A}\|_1 = Tr\left(\sqrt{(\Gamma^{T_A})^\dagger \Gamma^{T_A}}\right) \quad (7)$$

The negativity is an entanglement monotone [7] and, hence, it can be used as a measure of entanglement. It is null when the state is separable.

3. Quantum Entanglement Measures

When the state is a pure state, denoted by σ , the entanglement can be quantified by the von Neumann entropy of one of the individual parts of the system, $S = -Tr(\rho \log \rho)$, where $\rho = Tr_a \sigma = Tr_b \sigma$, being a and b the individual parts [4]. However, when the composite state is a mixed state, that we will call Γ , that is, a statistical mixture of pure states, the task to quantify the entanglement is harder. The first two measures proposed were the entanglement of formation, E_F , and the distillable entanglement, E_D [4]. The first one, E_F , is defined as the least expected entanglement of any ensemble of pure states realizing the mixed state whose entanglement we want to measure, $E_F(\Gamma) = \min \sum_i p_i S(|\sigma_i\rangle\langle\sigma_i|)$ such that $\Gamma = \sum_i p_i |\sigma_i\rangle\langle\sigma_i|$. The states $|\sigma_i\rangle$ are pure and not

necessarily orthogonal. The entanglement of formation can be calculated analytically by using Woottter's expression [5,6]:

$$E_F(\Gamma) = h \left[\frac{1 + \sqrt{1 - C^2(\Gamma)}}{2} \right] \quad (8)$$

$$h(x) = -x \log(x) - (1-x) \log(1-x) \quad (9)$$

$C(\Gamma)$ is the concurrence given by:

$$C(\Gamma) = \max[0, \lambda_1 - \lambda_2 - \lambda_3 - \lambda_4] \quad (10)$$

where $\lambda_{1,4}$ are the eigenvalues, in decreasing order, of the Hermitean matrix:

$$T = \sqrt{\sqrt{\Gamma} \tilde{\Gamma} \sqrt{\Gamma}} \quad (11)$$

In Eq. (11) $\tilde{\Gamma}$ is the spin flipped state:

$$\tilde{\Gamma} = (\sigma_y \otimes \sigma_y) \Gamma^* (\sigma_y \otimes \sigma_y) \quad (12)$$

$$\sigma_y = \begin{pmatrix} 0 & -i \\ i & 0 \end{pmatrix} \quad (13)$$

At last, Γ^* is the complex conjugated in the standard basis $\{|00\rangle, |01\rangle, |10\rangle, |11\rangle\}$. The distillable entanglement, E_D , is the maximal number of maximally entangled states that can be obtained, from a mixed entangled state, by using a purification protocol that involves local operations and classical communication between the parties, and its value depends on the protocol of purification used. Any other entanglement measure, obeying certain natural axioms, must be confined between E_F and E_D [8]. Among them, one of the most direct is the measure based on the relative entropy [9,10]. In order to calculate this measure, we need search the minimal relative entropy between the entangled state, whose entanglement we want to quantify, and all possible disentangled states. The relative entropy was introduced by Vedral and Plenio and, in a short way, can be described as follow [10]: The entanglement of a composite quantum state Γ can be given by the distance between this state and its nearest disentangled state:

$$E(\Gamma) = \min_{\rho \in d} D(\Gamma \| \rho) \quad (14)$$

where d is the set of all possible disentangled state. For the distance D , not necessarily a metric, we can use the quantum relative entropy, given by:

$$D(\Gamma \| \rho) \equiv S(\Gamma \| \rho) = Tr(\Gamma \ln \Gamma - \Gamma \ln \rho) \quad (15)$$

As we must search the solution among all possible disentangled states, we must use the most general formula of a disentangled state. For a bipartite state, in which we will concentrate our attention, this most general formula is [10]:

$$\rho = \sum_{i=1}^{16} p_i (\rho_a^i \otimes \rho_b^i) \quad (16)$$

where the coefficients p_i obey the normalisation condition:

$$\sum_{i=1}^{16} p_i = 1 \quad (17)$$

Finally, $\rho_{a,b}^i$ are pure states of the form:

$$\rho_a^i = \begin{bmatrix} \cos^2(\theta_i) & \cos(\theta_i)\sin(\theta_i)\exp(i\xi_i) \\ \cos(\theta_i)\sin(\theta_i)\exp(-i\xi_i) & \sin^2(\theta_i) \end{bmatrix} \quad (18)$$

$$\rho_b^i = \begin{bmatrix} \cos^2(\varphi_i) & \cos(\varphi_i)\sin(\varphi_i)\exp(i\phi_i) \\ \cos(\varphi_i)\sin(\varphi_i)\exp(-i\phi_i) & \sin^2(\varphi_i) \end{bmatrix} \quad (19)$$

The minimal distance, given by (15), can be obtained numerically using either the gradient method [10] or a genetic algorithm [11]. The most recent and easily computable quantum entanglement measure is the negativity given in (6), however, it is not based on asymptotic distillation and dilution of pure-state entanglement, like E_F , E_D and the measure based on relative entropy. Due to this, conversely those measures, it does not reduce to von Neumann entropy when applied to pure states [3].

4. Numerical Investigation of the Density Matrix

The main element to decide if the composite bipartite state is entangled or not, according Peres-Horodecki separability criterion and Vidal negativity, is the partial transpose of the density matrix. However, we can try to obtain information about the entanglement without use the partial transpose. Suppose, initially, a state Γ , which can be entangled or not, and whose individual parts are ρ_a and ρ_b . We can write this state as a sum of two matrices:

$$\Gamma = \rho_a \otimes \rho_b + R \quad (20)$$

where

$$R = \begin{pmatrix} k & q^* & p^* & x^* \\ q & -k & z^* & -p^* \\ p & z & -k & -q^* \\ x & -p & -q & k \end{pmatrix} \quad (21)$$

As we can see, the R matrix is Hermitean and it has null trace, hence, it does not represent a quantum state. Further, it has not influence in the density matrices of the individual parts. However, R influences strongly in the entanglement of the overall state. The amplitude of the elements of R must be such that the density matrix of the overall system, Γ , has not negative eigenvalues. The decomposition in (20) is not related with the decomposition proposed in [12]. In this one, a separable and, in general, not normalized matrix ρ_s is subtracted from Γ such that the matrix $\Gamma - \rho_s$ is still non-negative. If there exist a matrix ρ_s^* that has unitary trace and $\Gamma - \rho_s^*$ is still non-negative, then Γ is separable. In our case, the matrix that is subtracted from Γ is always normalized with trace equal to 1. Further, we do not require any condition to R matrix. Our investigations consist in search relations between properties of R , such as

determinant, eigenvalues, norms and singular values, and try to relate them to the entanglement of Γ . To test our hypotheses about the relations between those properties of R and the entanglement of the overall state Γ , we will use density matrices chosen randomly. Random density matrices for pure states can be obtained by [13]:

$$|\Psi\rangle = \begin{bmatrix} \cos(\varphi_3) \\ \sin(\varphi_3)\cos(\varphi_2)\exp(i\theta_3) \\ \sin(\varphi_3)\sin(\varphi_2)\cos(\varphi_1)\exp(i\theta_2) \\ \sin(\varphi_3)\sin(\varphi_2)\sin(\varphi_1)\exp(i\theta_1) \end{bmatrix} \quad (22)$$

$$\Gamma = |\Psi\rangle\langle\Psi| \quad (23)$$

where θ_k are random variables distributed uniformly in the interval $[0, 2\pi)$ while φ_k , belonging to the interval $[0, \pi/2]$, are obtained from the random variables ε_k , distributed uniformly in the interval $[0, 1]$, according to $\varphi_k = \arcsin(\varepsilon_k^{1/(2k)})$. On the other hand, random matrices of maximally entangled states, that is a particular class of pure states, are obtained by [13]:

$$|\Psi\rangle = \begin{bmatrix} \cos(\varphi_1)\exp(i\theta_1) \\ \sin(\varphi_1)\exp(i\theta_2) \\ -\sin(\varphi_1)\exp(-i\theta_2) \\ \cos(\varphi_1)\exp(-i\theta_1) \end{bmatrix} \quad (24)$$

$$\Gamma = |\Psi\rangle\langle\Psi| \quad (25)$$

Finally, an arbitrary density matrix Γ can be obtained by [14]:

$$\Gamma = UDU^+ \quad (26)$$

where U is an unitary matrix and D a diagonal matrix. The U matrix can be obtained from an ensemble of random unitary matrices produced in the following way [14-16]:

$$U = U^{(1,2)}(\phi_{12}, \psi_{12}, \theta_{12})U^{(2,3)}(\phi_{23}, \psi_{23}, 0)U^{(1,3)}(\phi_{13}, \psi_{13}, \theta_{13})U^{(3,4)}(\phi_{34}, \psi_{34}, 0) \\ U^{(2,4)}(\phi_{24}, \psi_{24}, 0)U^{(1,4)}(\phi_{14}, \psi_{14}, \theta_{14}) \quad (27)$$

where $U^{(i,j)}$, $i, j=1,2,3,4$, are complex matrices with three real parameters, ϕ, ψ and θ . Their rule of formation is:

$$U_{kl}^{(i,j)}(\phi, \psi, \theta) = \begin{cases} 1, & k=l, k \neq i, j \\ \sin(\phi)e^{i\theta}, & k=i, l=j \\ \cos(\phi)e^{i\psi}, & k=l=i \\ \cos(\phi)e^{-i\psi}, & k=l=j \\ -\sin(\phi)e^{-i\theta}, & k=j, l=i \\ 0, & \text{otherwise} \end{cases} \quad (28)$$

The angles ψ and θ are random variables uniformly distributed in the interval $[0, 2\pi)$, while the angles ϕ are obtained from $\phi_{ij} = \arcsin(\varepsilon^{1/(2i)})$, $i=1,2,3$, where ε is a random variable uniformly distributed in the interval $[0,1)$. At last, the diagonal matrix, D , has the following elements:

$$D_{11} = 1 - \xi_1^{1/3} \quad (29)$$

$$D_{22} = (1 - \xi_2^{1/2})(1 - D_{11}) \quad (30)$$

$$D_{33} = (1 - \xi_3)(1 - D_{11} - D_{22}) \quad (31)$$

$$D_{44} = 1 - D_{11} - D_{22} - D_{33} \quad (32)$$

where $\xi_{1,3}$ are also random variables distributed uniformly in the interval $[0,1)$. As mentioned before, the unitary matrices obtained using (27) and (28) are representative for the circular unitary ensemble. This ensemble consists of all unitary matrices with the natural Haar measure on the group $U(4)$ [15]. At last, (29)-(32) ensure the D 's elements are uniformly distributed on the manifold defined by $\sum_i D_{ii} = 1$.

Most of the mixed states produced using (26)-(32) are separable states. From numerical simulations it was estimated in [14] the probability of a created mixed state to be entangled is close to 0.365. In one simulation using only 20,000 states we found it equal to 0.3484.

4.1. Analysing Pure States

For each density matrix obtained using (22)-(23) the R matrix is obtained using:

$$R = \Gamma - Tr_b(\Gamma) \otimes Tr_a(\Gamma) \quad (33)$$

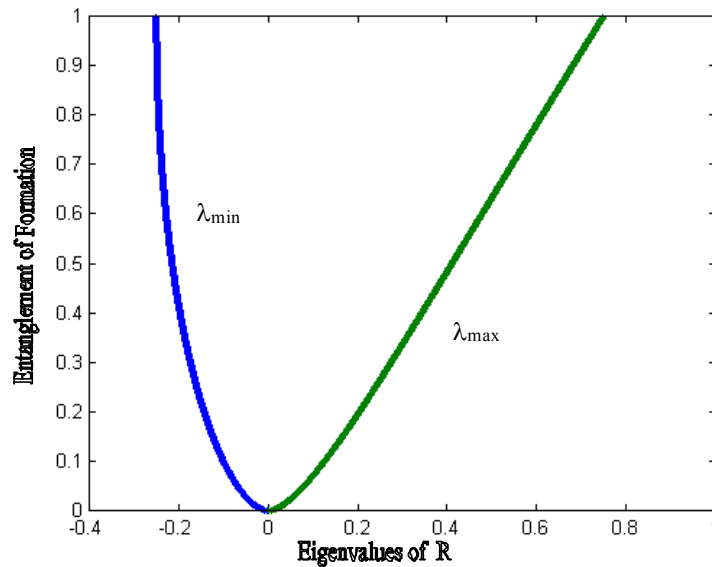


Fig. 1. Entanglement of formation (E_F) versus the maximum (λ_{\max}) and minimum (λ_{\min}) eigenvalues of R , for pure states obtained randomly.

For each density matrix chosen the entanglement of formation, E_F , is calculated using the Wootters' equation, (8)-(13). For pure states, strong correlations between the entanglement of Γ and the eigenvalues of R appear. In Fig. 1, we can see the relations between E_F and the minimum (λ_{\min}) and the maximum (λ_{\max}) eigenvalues of R . As can be observed in Fig. 1, the larger the absolute value of λ_{\min} and λ_{\max} the larger the entanglement.

It is interesting to analyse if the ordering induced by E_F is the same as the ordering induced by λ_{\min} and λ_{\max} . For this, we plot, in Fig. 2, ΔE_F versus $\Delta\lambda_{\min}$ and ΔE_F versus $\Delta\lambda_{\max}$, where ΔE_F , $\Delta\lambda_{\min}$ and $\Delta\lambda_{\max}$ are given by:

$$\Delta E_f(\Gamma_1, \Gamma_2) = \frac{E_f(\Gamma_1) - E_f(\Gamma_2)}{E_f(\Gamma_1) + E_f(\Gamma_2)} \quad (34)$$

$$\Delta\lambda_{\min(\max)}(\Gamma_1, \Gamma_2) = \frac{\lambda_{\min(\max)}(R_1) - \lambda_{\min(\max)}(R_2)}{\lambda_{\min(\max)}(R_1) + \lambda_{\min(\max)}(R_2)} \quad (35)$$

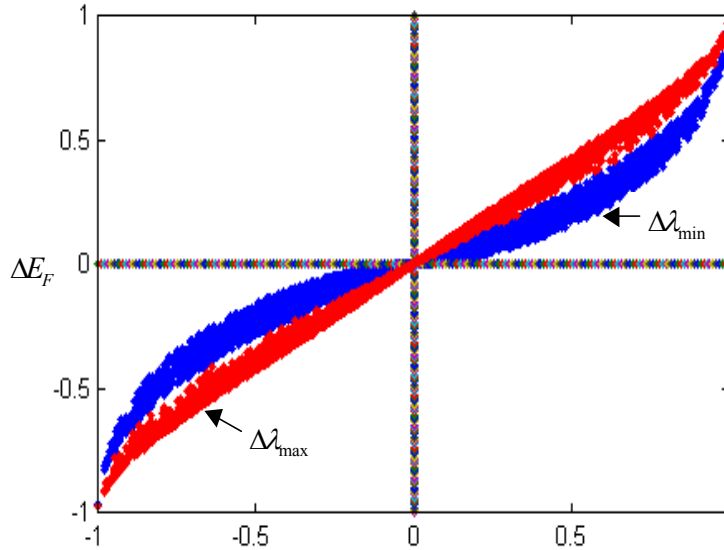


Fig. 2. ΔE_F versus $\Delta\lambda_{\max}$ and ΔE_F versus $\Delta\lambda_{\min}$ for 10.000 entangled pure states.

As we cannot find points in the second and fourth quadrant, we can see that the ordering induced by E_F , λ_{\min} and λ_{\max} is the same. It is easy to verify that the eigenvalues of R is related to the entanglement of bipartite pure states. An arbitrary bipartite pure state is described by Schmidt decomposition as $|\Psi\rangle = a|00\rangle + b|11\rangle$, where a and b are real non-negative numbers and $a^2 + b^2 = 1$. The concurrence (10), that is also an entanglement measure, of such states is $C(|\Psi\rangle\langle\Psi|) = 2a(1-a^2)^{1/2}$. Calculating the eigenvalues of R matrix for that class of states we obtain the following eigenvalues in decreasing order $\{C^2/4 + C/2, -C^2/4, -C^2/4, C^2/4 - C/2\}$. In Fig. 3 we can see R 's eigenvalues versus Concurrence.

Since all eigenvalues of R are well related to C , they can be used to measure the entanglement of pure bipartite states. However, we have to multiply the eigenvalues for a suitable constant like $4\lambda_{\max}/3$ or $-4\lambda_{\min}$ in order to have the entanglement measured varying from 0 to 1. The relations between the entanglement and some R 's properties are expected since a pure state is disentangled only if R is the null matrix.

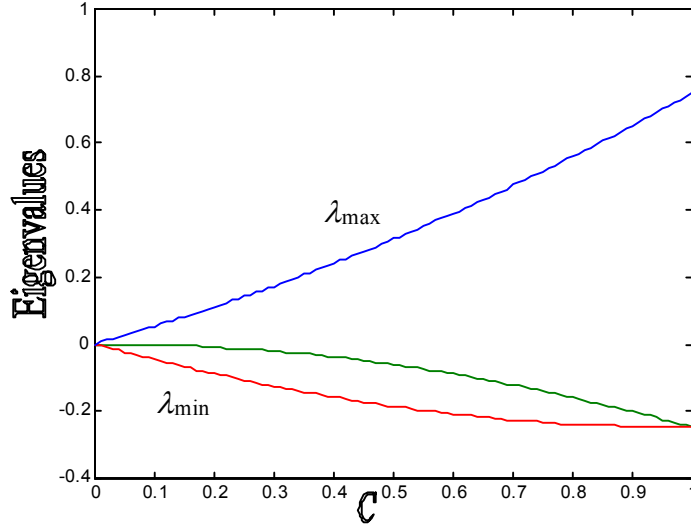


Fig. 3. Eigenvalues of R versus Concurrence for pure bipartite states of the form $|\psi\rangle=a|00\rangle+b|11\rangle$. $C=2a(1-a^2)^{1/2}$.

4.2. Analysing Mixed States

We choose the density matrices using (26)-(32) and the R matrix is obtained using (33). For each density matrix obtained, the Peres-Horodecki separability test is applied and the entanglement of formation, E_F , is evaluated using the Wootters's equation, (8)-(13). The problem for mixed states is much more hard. From all properties of R tested, the most interesting and the only one really important, was showed by the eigenvalue of R with maximal absolute value. In fact, based on the simulations, we can infer that, *if the eigenvalue of maximum absolute value of R has a negative sign or is zero, then the state is disentangled*. This can be seen in Fig. 4, where λ_{\max}^R is the eigenvalue of R with maximum absolute value and λ_{\min}^T is the minimum eigenvalue of the partial transposed of Γ .

In Fig. 4, using 20,000 points (states), we can observe that there are not entangled states ($\lambda_{\min}^T < 0$) for which λ_{\max}^R is negative, that is, the third quadrant is empty. Moreover, it seems to exist a forbidden region, that is, for each value of the λ_{\min}^T there is an upper bound to λ_{\max}^R and the boundary seems to be a straight line. Further, when the state is entangled, the larger the module of λ_{\min}^T the smaller the range of possible values of λ_{\max}^R . In Fig. 5 we plotted λ_{\max}^R versus E_F . As we can see in Fig. 5, there is a correlation between λ_{\max}^R and E_F , however, the ordering induced by E_F is different of the ordering induced by λ_{\max}^R , that is, $E_F(\Gamma_1) > E_F(\Gamma_2)$ does not necessarily imply $\lambda_{\max}^R(\Gamma_1) > \lambda_{\max}^R(\Gamma_2)$.

It is interesting to analyse the ordering question in a more restricted set of states. Suppose the states:

$$\Gamma_1 = \rho_a \otimes \rho_b + R_1 \quad (36)$$

$$\Gamma_2 = \rho_a \otimes \rho_b + R_2 \quad (37)$$

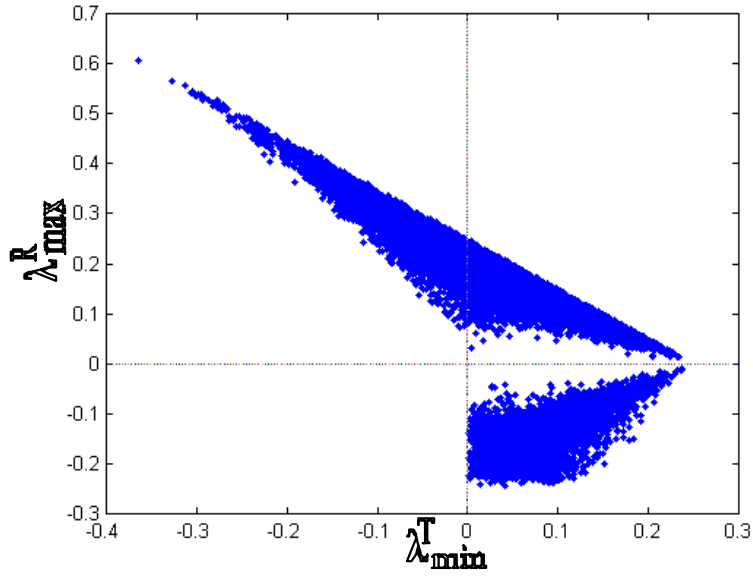


Fig. 4. Eigenvalue of maximum absolute value of R versus minimum eigenvalue of the partial transpose of Γ , for mixed states.

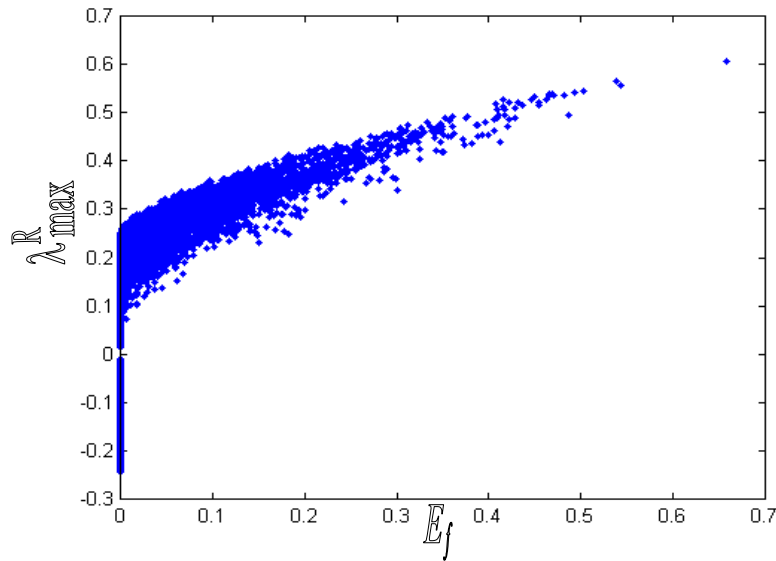


Fig. 5 – Eigenvalue of maximum absolute value of R versus entanglement of formation of Γ , for mixed states.

The difference between them is only the R matrix. Is the ordering induced by E_f the same for any property of $R_{1,2}$? Let us suppose, as a hypothesis, that the larger (lower) the norm of R , N (largest singular value of R), the larger (lower) the E_f . To test this, we generated, randomly, 23,660 states and we calculated:

$$\Delta E_F(\Gamma_1, \Gamma_2) = \frac{E_F(\Gamma_1) - E_F(\Gamma_2)}{E_F(\Gamma_1) + E_F(\Gamma_2)} \quad (38)$$

$$\Delta N(\Gamma_1, \Gamma_2) = \frac{N(R_1) - N(R_2)}{N(R_1) + N(R_2)} \quad (39)$$

The plot of ΔE_F versus ΔN can be seen in Fig. 6. In Fig. 6 we can observe the presence of states in the second and fourth quadrants, what imply that, even in the restricted set of states given by (36)-(37), the ordering induced is not the same, as well as the ordering induced by E_F and $|\lambda_{\min}^T|$ is not the same, as can be seen in Fig. 7 [14], with $\Delta\lambda$ given by:

$$\Delta\lambda(\Gamma_1, \Gamma_2) = \frac{|\lambda_{\min}^T(\Gamma_1)| - |\lambda_{\min}^T(\Gamma_2)|}{|\lambda_{\min}^T(\Gamma_1)| + |\lambda_{\min}^T(\Gamma_2)|} \quad (40)$$

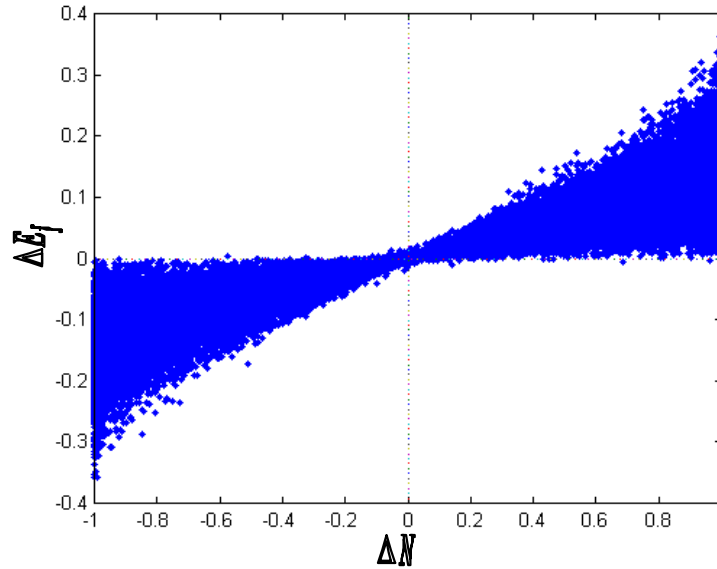


Fig. 6. ΔE_F versus ΔN for 23,660 entangled mixed states.

In fact, for mixed states none of the properties of R tested conserved the order induced by E_F . It is also interesting to know if the decomposition (20) is the one that give us most information about the entanglement of the state. This is not easy to answer since infinite decompositions are allowed. We will test now another decomposition. Suppose the states:

$$\Gamma_1 = \rho_a \otimes \rho_b + R \quad (41)$$

$$\Gamma_2 = \sum_i \rho_a^i \otimes \rho_b^i + R \quad (42)$$

where

$$\text{Tr}_a \left(\sum_i \rho_a^i \otimes \rho_b^i \right) = \rho_b \tag{43}$$

$$\text{Tr}_b \left(\sum_i \rho_a^i \otimes \rho_b^i \right) = \rho_a \tag{44}$$

Hence, the disentangled state in the decomposition can be a product state, (41), or a separable state, (42). In both the R matrix is the same. In Fig. 8 we have, for Γ_1 and Γ_2 , the plot of λ_{\max}^R versus λ_{\min}^T .

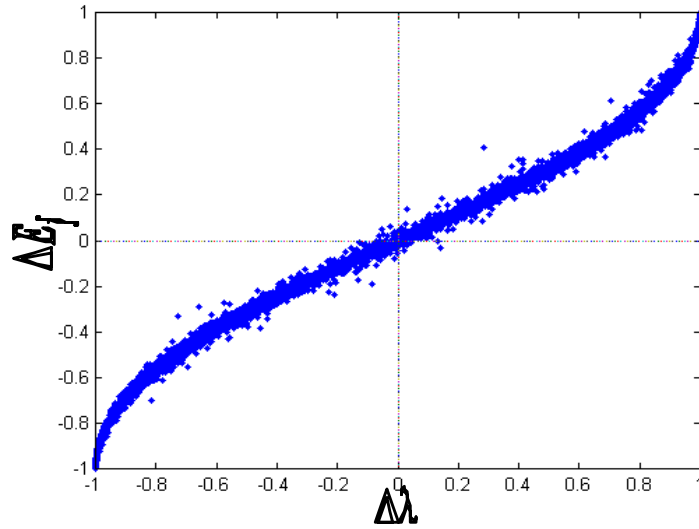


Fig. 7. ΔE_f versus $\Delta \lambda$ for 23,660 entangled mixed states.

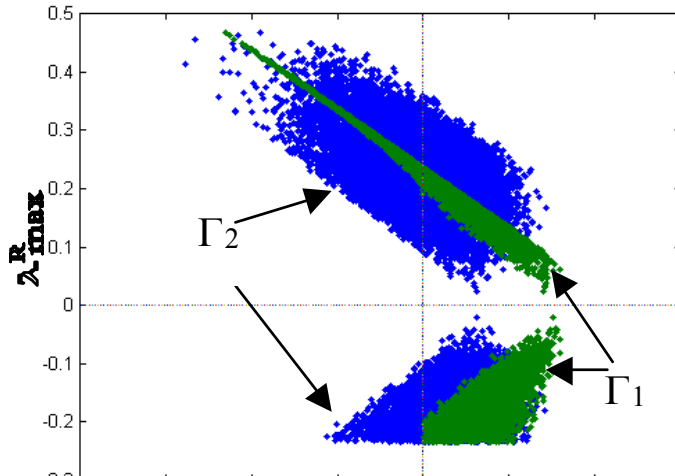


Fig. 8. Eigenvalue of maximum absolute value of R versus minimum eigenvalue of the partial transpose of Γ , for mixed states. $\Gamma_1 \rightarrow$ Eq. (41) and $\Gamma_2 \rightarrow$ Eq. (42).

As can be observed in Fig. 8, for the state Γ_2 , if the eigenvalue of R of maximum absolute value is negative the state is not necessarily disentangled. We also cannot see the forbidden region shown in Fig. 4. In fact, the data for Γ_2 are more diffused.

5. Disentanglement

Now we will use the matrix R in a different problem: the disentanglement [17-19]. The disentanglement process consists in erasing the entanglement of a composite system, while leaving its individual parts intact. Let M to be a completely positive linear map preserving the trace of the state:

$$\Phi = M\Gamma \tag{45}$$

then, for the initial and final states we have the same individual parts:

$$\rho_a = Tr_b(\Gamma) = Tr_b(\Phi) \tag{46}$$

$$\rho_b = Tr_a(\Gamma) = Tr_a(\Phi) \tag{47}$$

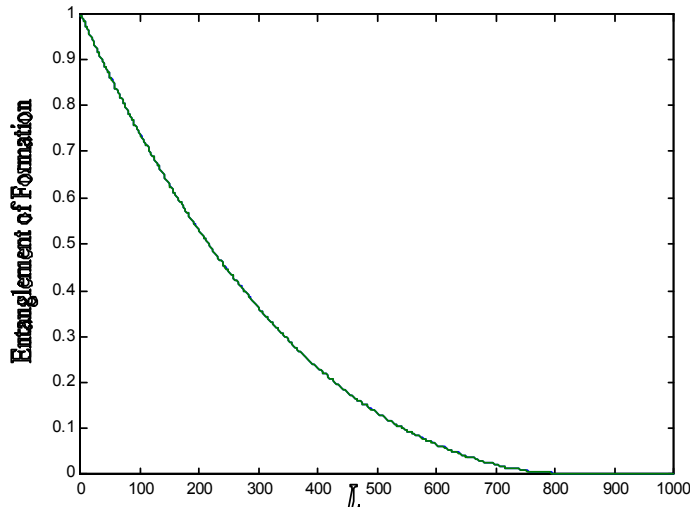


Fig. 9. Evolution of the entanglement of formation during the propagation in the bistochastics channel B_1 .

Since the final state Φ is disentangled it can be a product state $\Phi = \rho_a \otimes \rho_b$ or a separable state $\Phi = \sum_i p_i \rho_a^i \otimes \rho_b^i$. Our decomposition, (20)-(21), is very suitable to study the disentanglement, since

any disentangling procedure will act only in the R matrix, leaving the first term on the right side of (20) intact. Mathematically we can work with the elements of R in order to disentangle Γ . Let us firstly consider a natural disentangling machine: a noisy quantum channel. We will use the bistochastic channel defined in [13]:

$$\Phi \equiv B(\Gamma) = \sum_{i=1}^4 p_i \sigma_i \Gamma \sigma_i^+ \quad (48)$$

$$\sum_{i=1}^4 p_i = 1 \quad (49)$$

where σ_{1-4} are the Pauli matrices. The bistochastic quantum channel increases the entropy of the individual parts leaving them towards to maximally mixed states. Hence, in order to preserve the individual parts of the overall state during the propagation in the channel, the states considered are maximally entangled states chosen randomly according to (24)-(25). The individual parts of these states are the maximally mixed states $\rho_a = \rho_b = 0.5 * I$, where I is the identity matrix. For simplicity, only one subsystem will be sent through the bistochastic channel. Let us consider firstly the channel B_1 with the parameters: $p_1 = (1-e)$, $p_2 = p_3 = p_4 = e/3$, with $0 \leq e \leq 1$. Using $e = 0.001$ we obtain the curve for E_F shown in Fig. 9.

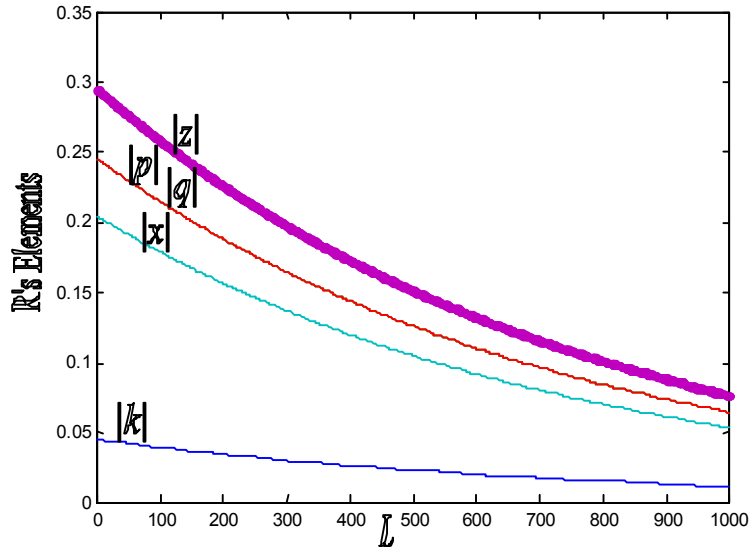


Fig. 10. Evolution of the absolute value of the R 's elements during the propagation in the bistochastics channel B_1 .

Their angles are not changed during propagation. As we can see in Figs. 9 and 10, the entanglement of formation and the absolute value of R 's elements decay exponentially. Further, they fall off with the same velocity. In fact, those curves are very well fitted by $\exp(-1.335 eL)$, where L is the "distance of propagation" in the quantum channel. The error is close to 10^{-4} . The curves in Figs. 9 and 10 are equal for any initial maximally entangled state. Hence, the propagation of a maximally entangled state in the channel B_1 can be simply modelled by:

$$\Phi(L) = Tr_b(\Gamma) \otimes Tr_a(\Gamma) + R \exp(-1.335eL) \quad (50)$$

where Γ is the initial maximally entangled state and $\Phi(L)$ is the state in the "position" L . Let us call L_D the distance in which the state Φ becomes disentangled, $E_F[\Phi(L_D)] = 0$. Then, for the channel B_1 , the relative entropy, between Γ and $\Phi(L_D)$ is $S(\Gamma \parallel \Phi(L_D)) \approx 1.0005679$. The relative entropic distance (15) $S(\Gamma \parallel \Phi(L_D))$ depends on the value of e . Let us consider now the channel B_2 with parameters: $p_1 = (1-e)$,

$p_2 = 0, p_3 = p_4 = e/2$, with $0 \leq e \leq 1$. Using $e = 0.001$ we obtain the plot for E_F shown in Fig. 11. In Fig. 12 we plot the absolute value of R 's elements. Their angles are not changed during propagation.

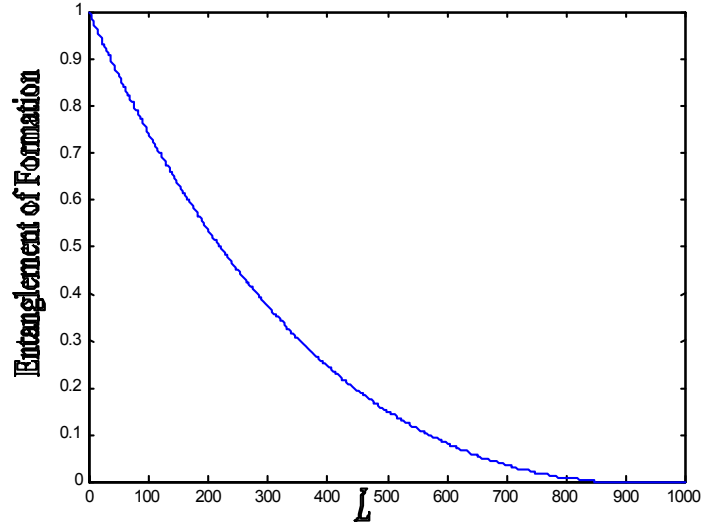


Fig. 11. Evolution of the entanglement of formation during the propagation in the bistochastics channel B_2 .

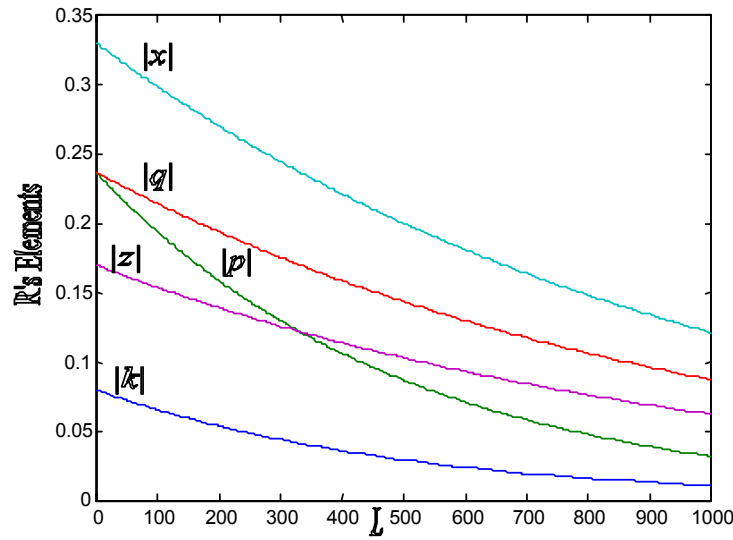


Fig. 12 – Evolution of the absolute value of the R 's elements during the propagation in the bistochastics channel B_2 .

E_F decays, as expected, but not exponentially. On the other hand, the absolute values of R 's elements decay exponentially but with different velocities. The curves for $|k|$ and $|p|$ are well fitted by $\exp(-2eL)$, while the curves for $|q|$, $|z|$ and $|x|$ are well fitted by $\exp(-eL)$. The errors are close to 10^{-4} . Hence, the propagation of maximally entangled states in the channel B_2 is modelled by:

$$\Phi(L) = Tr_b(\Gamma) \otimes Tr_a(\Gamma) + e^{-eL} \begin{bmatrix} ke^{-eL} & p^* e^{-eL} & q^* & x^* \\ pe^{-eL} & -ke^{-eL} & z^* & -q^* \\ q & z & -ke^{-eL} & -p^* e^{-eL} \\ x & -q & -pe^{-eL} & ke^{-eL} \end{bmatrix} \quad (51)$$

The relative entropy between Γ and $\Phi(L_D)$, for the second channel used, is $S(\Gamma \|\Phi(L_D)) \approx 1.0001659$.

At last, we did several simulations choosing the channel's parameters randomly, using (29)-(32). We found that the absolute values of k and p always fall off with the same velocity. The same occurred to the absolute values of z , x and q . Hence, in general, for maximally entangled states, the entanglement during propagation in the bistochastic channel does not decay exponentially. In the especial case when $p_2 = p_3 = p_4$ it does.

6. R Matrix and Relative Entropy

Here we investigate what is the importance of the relative entropy between an entangled state and a disentangled (product) state with the same individual parts. Let us introduce the two relatives entropies that will be used.

$$S_1 = S(\Gamma \|\Phi) \quad (52)$$

where

$$\Phi = Tr_b(\Gamma) \otimes Tr_a(\Gamma) + R \exp(-\alpha) \quad (53)$$

and

$$S_2 = S(\Gamma \|\Tr_b(\Gamma) \otimes Tr_a(\Gamma)) \quad (54)$$

where α is the minimal value for what the state Φ becomes disentangled. For a pure state the entanglement of formation (or von Neumann entropy of the individual parts) can be approximated by $0.5S_2$. We did several simulations, choosing pure states randomly according to (22)-(23), and one of them is shown in Fig. 13. In this picture we plot E_F , circles (o), S_1 , points (·), and $0.5S_2$, crosses (+), for only 100 states for better visualisation.

As we can observe in Fig. 13, $0.5S_2$ fits E_F very well. For mixed states (52) can be used as a first approximation for the closest disentangled state of Γ . This is useful in algorithms to calculate the entropy measure based on the relative entropy, which require a minimisation procedure. Since (52) is a good start point, the time of search of the algorithm of minimisation tends to decrease. To have an idea of how good it can be, let us consider now the following family of states introduced in Ref. 20:

$$\Gamma = g|\Psi_1\rangle\langle\Psi_1| + (1-g)|\Psi_2\rangle\langle\Psi_2| \quad (55)$$

$$|\Psi_1\rangle = a|00\rangle + \sqrt{1-a^2}|11\rangle \quad (56)$$

$$|\Psi_2\rangle = a|10\rangle + \sqrt{1-a^2}|01\rangle \quad (57)$$

where $0 < g, a < 1$ and the states $|00\rangle, |01\rangle, |10\rangle$ and $|11\rangle$ form the standard basis. The density matrix, (55), in the standard basis is:

$$\Gamma = \begin{bmatrix} ga^2 & 0 & 0 & ga\sqrt{1-a^2} \\ 0 & (1-g)(1-a^2) & (1-g)a\sqrt{1-a^2} & 0 \\ 0 & (1-g)a\sqrt{1-a^2} & (1-g)a^2 & 0 \\ ga\sqrt{1-a^2} & 0 & 0 & g(1-a^2) \end{bmatrix} \quad (58)$$

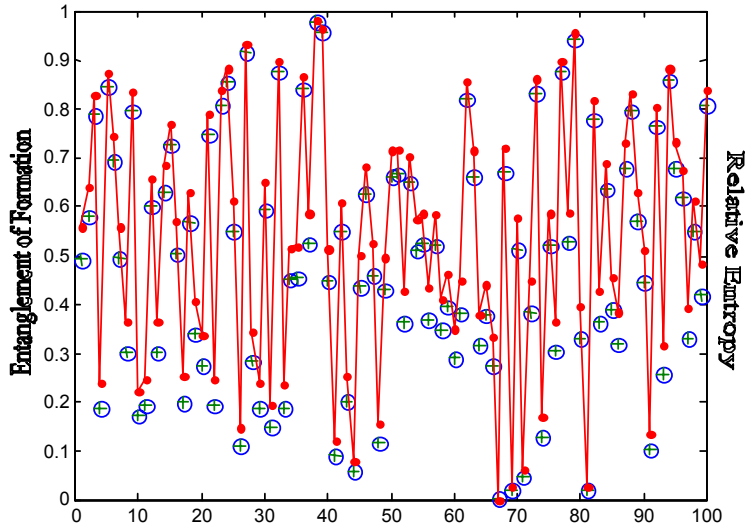


Fig. 13. Entanglement of formation (E_F) and relative entropies S_1 and S_2 for 100 pure states chosen randomly.

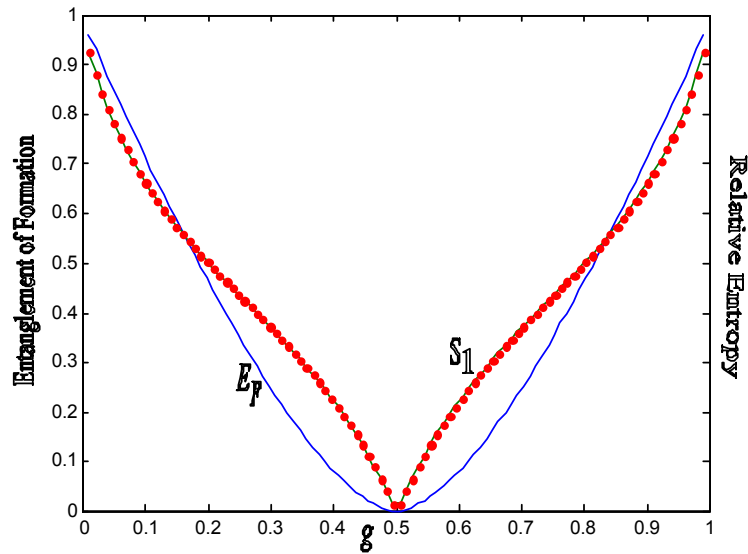


Fig. 14. Entanglement of formation (E_F) and relative entropy S_1 for the class of states in (58) with $a = 0.75$.

In Fig. 14, we show the entanglement of formation (continuous line), E_F , and the relative entropy S_1 (dotted line), for the state in (58). In this simulation we use $a = 0.75$ and g varying in the interval $(0,1)$. As we can see in Fig. 14, S_1 is reasonably close to E_F implying that (52) is a good starting point for an algorithm to calculate the entanglement based on the relative entropy, like the one used in [11].

7. Conclusions

We proposed a different approach to treat the density matrix aiming to obtain information about the entanglement. We separated the density matrix in a sum of two other matrices: one representing a disentangled state, which is responsible for the individual parts of the overall state, and the other, called R , being only the rest. We have found, numerically and analytically, for pure states, that the eigenvalues of R are directly related to the concurrence of the overall state. Hence, for pure states, we can measure the entanglement using the eigenvalues of R . For mixed states we can find out if a state is disentangled looking at the signal of the eigenvalue of R of maximal absolute value. If it is negative or null, then the state is disentangled otherwise nothing can be inferred. For mixed states, none of the parameters of R that we tested preserve the order induced by the entanglement of formation, hence, they are not useful. We also tested another decomposition, equation (42), for the density matrix but it did not show the same property of the decomposition given by equation (20). Following, we analysed how the R 's elements change during the disentanglement caused by a bistochastic channel. The magnitude of R 's elements decay exponentially with two different velocities, one for $|k|$ and $|p|$, and other for $|q|$, $|x|$ and $|z|$. Hence, in general, for bistochastic channels, the entanglement does not fall off exponentially during the disentanglement process preserving the individual parts. At last, we found that the entanglement of pure bipartite states can be approximated by the half of the relative entropy of the entangled state and the product state of its individual parts. Further, the state disentangled obtained by the exponential decay of the R 's elements can be used as a good starting point in algorithms to perform the minimisation required by the measure of entanglement based on the relative entropy.

Acknowledgements

This work was partially supported by the Brazilian agency CAPES and the Swedish Technical Science Research Council (TFR).

References

1. Asher Peres (1996), *Separability Criterion for Density Matrices*, Phys. Rev. Lett., 77, 8, pp. 1413-1415.
2. Michal Horodecki, Pawel Horodecki and Ryszard Horodecki (1996), *Separability of mixed states: necessary and sufficient conditions*, Phys. Lett. A, 223, pp. 1-8.
3. G. Vidal and R. F. Werner (2001), *A computable measure of entanglement*, quant-ph/0102117.
4. C. H. Bennet, D. P. DiVincenzo, J. A. Smolin, and W. K. Wootters (1996), *Mixed-state entanglement and quantum error correction*, Phys. Rev. A, 54, pp. 3824-3851.
5. Scott Hill and William K. Wootters (1997), *Entanglement of a Pair of Quantum Bits*, Phys. Rev. Lett., 78, 26, pp. 5022-5025.
6. William K. Wootters (1998), *Entanglement of Formation of an Arbitrary State of Two Qubits*, Phys. Rev. Lett., 80, 10, pp. 2245-2248.
7. G. Vidal (2000), *Entanglement monotones*, J. Mod. Opt., 47, pp. 355-376.
8. Michal Horodecki, Pawel Horodecki and Ryszard Horodecki (1999), *Limits for entanglement measures*, quant-ph/9908065.
9. V. Vedral, M. B. Plenio, M. A. Ripping, and P. L. Knight (1997), *Quantifying Entanglement*, Phys. Rev. Lett., 78, pp. 2275-2279.
10. V. Vedral and M. B. Plenio (1998), *Entanglement measures and purification procedures*, Phys. Rev. A, 57, 3, pp. 1619-1633.
11. Rubens V. Ramos and Rui F. Souza (2002), *Calculation of the quantum entanglement measure of bipartite states, based on relative entropy, using genetics algorithms*, J. Comp. Phys., 175, pp. 576-583.

12. Macej Lewenstein and Anna Sanpera, *Separability and entanglement of composite quantum systems*, quant-ph/9707043.
13. Karol Zyczkowski, Pawel Horodecki, Michal Horodecki and Ryszard Horodecki (2000), *Dynamics of quantum entanglement*, quant-ph/0008115.
14. Jean Eisert and Martin B. Plenio (1999), *A Comparison of Entanglement Measures*, quant-ph/9807034.
15. Karol Zyczkowski and Marek Kus (1994), *Random unitary matrices*, J. Phys. A: Math. Gen., 27, pp. 4235-4245.
16. Marcin Pozniak, Karol Zyczkowski and Marek Kus (1998), *Composed ensembles of random unitary matrices*, J. Phys. A: Math. Gen., 31, pp. 1059-1071.
17. Daniel R. Terno (1999), *Nonlinear operations in quantum-information theory*, Phys. Rev. A, 59, pp. 3320-3324.
18. Tal Mor (1998), *On the Disentanglement of States*, quant-ph/9812020.
19. Tal Mor and Daniel Terno (1999), *Sufficient conditions for a disentanglement*, quant-ph/9907036.
20. R. Horodecki (1996), *Two-spin- $\frac{1}{2}$ mixtures and Bell's inequalities*, Phys. Lett. A, 210, pp. 223.